JOURNAL OF MATERIALS SCIENCE **40** (2005) 2923–2930

Crystallographic and low frequency conductivity studies of the spinel systems $CuFe_2O_4$ and $Cu_{1-x}Zn_xGa_{0.1}Fe_{1.9}O_4$; $(0.0 \leq x \leq 0.5)$

S. S. ATA-ALLAH, F. M. SAYEDAHMED, M. KAISER, A. M. HASHHASH
Reactor and Neutron Physics Department, Nuclear Research Center, Atomic Energy Authority, Cairo, Egypt

Spinel solid solutions of $CuFe_2O_4$ and $Cu_{1-x}Zn_xGa_{0.1}Fe_{1.9}O_4$ with $(0.0 \leq x \leq 0.5)$ are synthesized. Crystallographic phase transformation from tetragonal-to-cubic occurred at $x = 0.2$. The derived structural parameters manifest that Zn occupies the tetrahedral *A*-site while Cu and Ga occupy the octahedral *B*-site and Fe distributes among *A*- and *B*-sites. Electrical conductivity measurements of these materials as a function of temperature and frequency revealed semiconducting behavior except $CuFe_2O_4$ sample, which has a metallic behavior at low frequency and at high frequency, semiconductor-to-metallic transition occurred as temperature increases. The metallic behavior in this sample is attributed to cation-cation interactions at *B*-site while, the semiconductor behavior in $Cu_{1-x}Zn_xGa_{0.1}Fe_{1.9}O_4$ compounds is due to the cation–anion–cation interactions at the same site in the spinel lattice. All compositions exhibit transition with change in the slope of conductivity versus temperature curve. This transition temperature (T_c) decreases linearly with increasing Zn content *x*. The relation of the universal exponent *s* with temperature gives evidence that over large polaron OLP and correlated barrier hopping CBH conduction mechanisms are presented in $CuFe_2O_4$ and $Cu_{1-x}Zn_xGa_{0.1}Fe_{1.9}O_4$ compounds respectively.

1. Introduction

Many ferrites have the spinel-type structure [1, 2] which can be described in terms of a nearly cubic close-packed arrangement of anions with one-half of the octahedral interstices (*B*-sites) and one-eighth of the tetrahedral interstices (*A*-sites) filled with cations, the space group being Fd3 m. The general formula of compounds with the spinel structure is AB_2O_4 and there are eight of these units in a unit cell. In the non-ideal structure the anions are displaced from their ideal positions along [directions away from the nearest tetrahedral hole]. This deviation is quantified by the oxygen parameter, u, which is 0.375 in the ideal structure, but very often takes significantly higher values [1, 3, 4].

The study of transition metal oxides (TMO), especially spinel ferrites is of great importance from both fundamental and applied research points of view [5, 6]. The characteristic physical properties of the spinel ferrites (e.g., electric and magnetic properties) arise from the ability of these compounds to distribute the cations amongst the available tetrahedral *A*- and octahedral *B*-sites [7, 8]. $ZnFe_2O_4$ is an example for a normal spinel where Zn ions are occupying the *A*-site, Fe ions are at *B*-sits, and $CuFe_2O_4$ is an inverse spinel where Cu ions are at *B*-sites and Fe ions distributed equally between *A*- and *B*-sites [9]. Due to the Jahn-Teller (JT) effect, many TM compounds show a more or less strong deviation from their ideal crystal structure. Examples can be found in the spinel and the perovskite family [10]. The copper compounds are very special due to JT distortion of CuO_6 octahedron [11]. The JT distortion in copper ferrospinel has established that the critical number of octahedral site Cu^{2+} ions per formula unit for a cooperative distortion to tetragonal symmetry at room temperature is 0.8 [9]. The aim of the present work is to study the effect of Zn doping on the crystal structure and frequency dependence of conductivity for the spinel systems $CuFe_2O_4$ and $Cu_{1-x}Zn_xGa_{0.1}Fe_{1.9}O_4$ $(0.0 \leq x \leq 0.5)$. In addition, the role of direct and indirect interactions between cations and anions over the octahedral *B*-sites in these compounds aimed to be clarified.

2. Experimental

The studied compounds $CuFe_2O_4$ and $Cu_{1-x}Zn_xGa_{0.1}Fe_{1.9}O_4$ with *x* ranges from 0.0 to 0.5 are prepared by solid-state reactions using CuO, Fe_2O_3, Ga_2O_3 and ZnO (with purity ≥99.99%) as starting materials. The mixture of the oxide powders is prefired at (950–1100°C) depending on the CuO content for 24 h. The product is reground and fired again at the same conditions to improve homogeneity. The final powders are pressed into pellets and sintered at (1000–1200°C) for 8 h, then slowly cooled to room temperature. X-ray powder diffraction (XRD) measurements are

obtained using Cu K_α radiation and their analysis showed that the products are crystallized in single-phase spinel with tetragonal unit cell for $CuFe_2O_4$, $CuGa_{0.1}Fe_{1.9}O_4$ and $Cu_{0.9}Zn_{0.1}Ga_{0.1}Fe_{1.9}O_4$ and cubic unit cell for samples with $0.2 \leq x \leq 0.5$. It is usually accepted; based on the criticism that the reliability of X-ray diffraction methods with respect to the solution of the exact cation distribution between *A*- and *B*-sites in the spinel structure of ferrites generally not great compared with neutron diffraction method. However, if there is a sufficient difference of atomic number between the cations resent in the spinel structure. The reliability of the measured characteristic parameters [i.e., the cation distribution and the oxygen positional parameter, *u*] strongly depends on the precision of the observed X-ray line intensities and on the theoretical data used for the scattering model of the system. The electrical measurements are carried out on the prepared samples in the form of pellets with surfaces coated with silver paste to ensure good electrical contact and with dimensions of (∼1 cm in diameter ∼4 mm in thickness) using two-probe method with the applying of a complex impedance technique. Where, SR510 Lock-in amplifier is used to measure the voltage difference (V_R) between the two ends of known resistance *R* which is connected in series with the sample (in an equivalent RC circuit) in the frequency range (10^2–10^5 Hz). The value of *R* is adjusted such that V_R is very small (less than 1%) compared with the value of the applied voltage *V* across the sample [the root mean square (r.m.s.) value of $V = 1$ volt]. The current *I* passes through the sample has two components. The conductivity σ is calculated from the in-phase component ($I \cos\theta$) using the formula; $\sigma = I \cos\theta\ (d/A)$ and $I = V_R/R$, where, *d* is the thickness of the sample, A is the cross-sectional area, θ is phase difference between *V* and *I*. Samples were kept under vacuum (∼1.3×10^{-4} Pa) during the measurements.

3. Results and discussion

Fig. 1 shows the XRD patterns of the prepared samples $CuFe_2O_4$ and $Cu_{1-x}Zn_xGa_{0.1}Fe_{1.9}O_4$ with ($0.0 \leq x \leq 0.5$). The diffraction peaks are fitted by modified Gaussian functions. The result of indexing XRD patterns shows that the nominal composition structures with different concentration are single phase with no additional lines corresponding to any other phases, where the lattice parameters are obtained from the fitting of the diffracted peaks.

Tetragonal structure is obtained for $CuFe_2O_4$, $CuGa_{0.1}Fe_{1.9}O_4$ and $Cu_{0.9}Zn_{0.1}Ga_{0.1}Fe_{1.9}O_4$ with $c/a > 1$ as shown in Table I. This can be explained as; the metal sites in most TMO system have octahedral site symmetry (D_h), in which each TM ions Cu is surrounded by six oxygen ions, MO_6, and the TM ion becomes tetragonal (D_{4h}) due to the lattice distortion with the elongation of the out-of-phase M─O bonding lengths and the shortening of the in-plane M─O one [9]. The cooperative nature of the crystal distortions in these compounds can be rationalized in terms of elastic interactions between the locally distorted polyhedra.

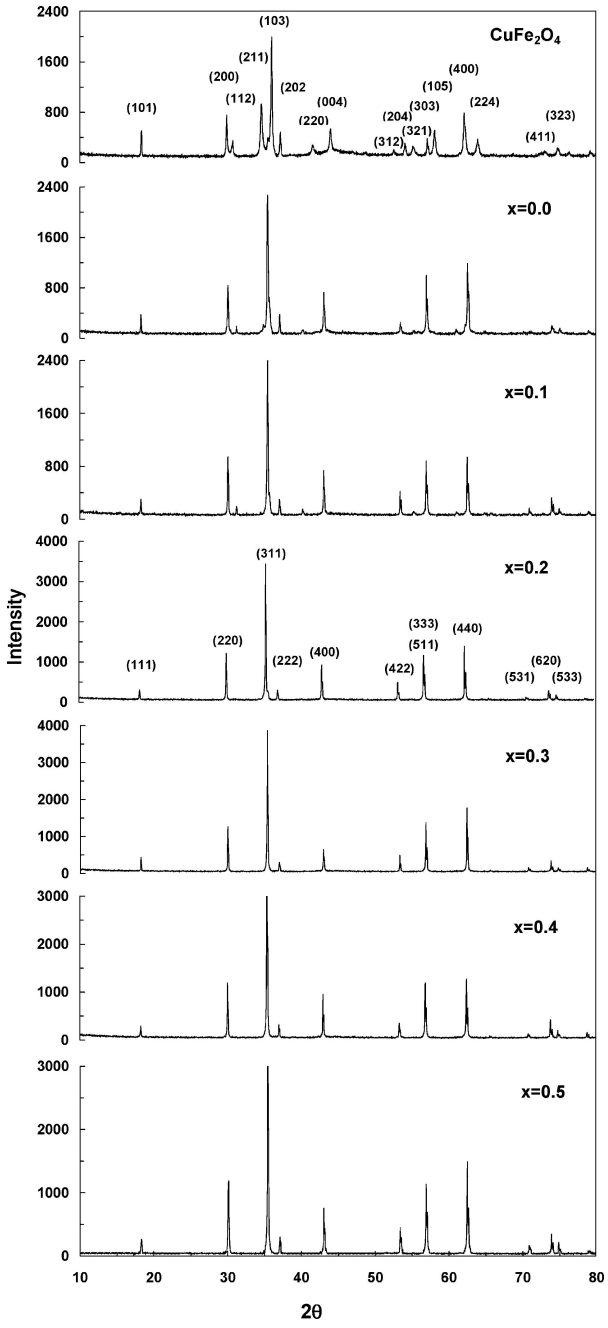

Figure 1 XRD patterns for $CuFe_2O_4$ and $Cu_{1-x}Zn_xGa_{0.1}Fe_{1.9}O_4$ at room temperature.

Statistical theories of such distortions in spinels (octahedral sites) [13–16] demonstrate that tetragonal structures result from parallel alignments of tetragonally distorted polyhedra in a cubic unit cell. This agrees with the values of the *c* parameter in the tetragonal unit cell which are close to the values of the lattice parameter *a* of the cubic unit cell as given in Table I.

In the present study, the tetragonal distortion in $CuFe_2O_4$, $CuGa_{0.1}Fe_{1.9}O_4$ and $Cu_{0.9}Zn_{0.1}Ga_{0.1}Fe_{1.9}O_4$

TABLE I Lattice parameters for samples with tetragonal unit cell

Sample	*c* (Å)	*a* (Å)	*c*/*a*
$CuFe_2O_4$	8.2245(6)	5.9694(8)	1.366
$CuGa_{0.1}Fe_{1.9}O_4$	8.3748(2)	6.1285(3)	1.377
$Cu_{0.9}Zn_{0.1}Ga_{0.1}Fe_{1.9}O_4$	8.3938(3)	6.1363(4)	1.368

TABLE II Determined structure parameters for samples with cubic cell for the spinel $Cu_{1-x}Zn_xGa_{0.1}Fe_{1.9}O_4$ series. The reliability R was calculated using 13 reflections

x	$\langle a \rangle$ Å	U $\pm$ 0.001	Fe $_B$ $\pm$ 0.005	R
0.2	8.3838(8)	0.384	1.11	0.022
0.3	8.3850(6)	0.385	1.20	0.017
0.4	8.3998(2)	0.385	1.32	0.019
0.5	8.4074(7)	0.385	1.41	0.024

compounds is attributed to the cooperative distortion that driven by the octahedral Cu^{2+} ($3d^9$). As Zn^{2+} substitutes Cu^{2+} in this system, it replaces Fe^{3+} at A-site [9]. This is due to the site preference of Zn^{2+} [9] which leads to transfer Fe^{3+} from A-site to B-sites and in turns a crystallographic transformation from tetragonal to cubic structure is occurred at ($x \geq 0.2$ as shown in Fig. 1). This crystallographic transformation is attributed to the decrease of the concentration of the JT ions [Cu^{2+} ($3d^9$)] in the host structure at the octahedral sites because of Zn substitution and leads to a high-symmetry phase (the cubic phase).

The determined lattice parameter a for samples with cubic unit cell at different compositional parameter x is given in Table II, where a increases with increasing Zn concentration. This is due to the fact that Pauling ionic radius of Zn^{2+} (0.74 Å) is greater than that of Cu^{2+} (0.72 Å).

The intensity for each diffraction peak in the XRD patterns is given by

$$I_{hkl}(2\theta) = \frac{\alpha_{hkl}\sin(\pi/\alpha_{hkl})}{\pi\Gamma_{hkl}} \frac{I_{hkl}}{1+\left|\frac{2(2\theta-2\theta_{hkl}}{\Gamma_{hkl}}\right|^{\alpha_{hkl}}} \qquad 1$$

where the adjustable parameters for each diffraction peak are the Integrated intensity I_{hkl}, the full width at half maximum (FWHM) Γ_{hkI}, the position 2θ and the exponent α_{hkl}. An exponential factor in 2θ was incorporated into Equation 1 to account for the curvature of the background at low angles.

To derive the cation distribution from the obtained integral intensities, the Lorentz polarization factor, the average Debye-Waller temperature factor, the atomic scattering factors as a function of $\sin\theta/\lambda$ are corrected for anomalous dispersion (for numerical values, see International Tables for X-ray Crystallography, Vol. IV, 1974). The multiplicity factor and the atomic positions have been taken into account for the calculation of the reflection intensities [17]. Oxygen parameter u and cation distribution parameters have been allowed to vary during a non-linear least squares minimization of the reliability factor R [18, 19].

An example of step scan XRD pattern is shown in Fig. 2. The analysis of the line profiles revealed that the FWHM ranged from 0.17° at two diffraction angles to 0.24° at high diffraction angles and that the exponent α_{hkl} in equation 1 had an average value of 2.5, irrespective of the investigated samples. These values indicate a relatively high degree of crystallinity for the involved samples.

The evaluation of the octahedral Ga content was not straightforward. Generally, it is not possible to distinguish between transition metal ions differing by not more than a small number of electrons. The atomic scattering factors of Fe and Zn, after correction for anomalous dispersion, are not sufficiently different from each other to have a marked effect on the calculated intensities of the diffraction peaks and consequently, distinguishing between Fe and Zn is not possible. Knowing the strong preference of Zn for four-fold coordination, one could assume that all Zn ions occupy tetrahedral sites. Therefore, only the distribution of the Ga and Fe ions between both sites could be derived from the XRD spectra with some accuracy. The results are tabulated in Tables II and III.

Fig. 3 shows the variation of conductivity as ($\ln\sigma$) with reciprocal of temperature as ($1000/T$) at different frequencies for the synthesized $CuFe_2O_4$ and $Cu_{1-x}Zn_xGa_{0.1}Fe_{1.9}O_4$ samples. Results in this figure reveal that for $CuFe_2O_4$ sample, at low frequency regime, metallic behavior of conductivity σ with temperature is observed (where, σ decreases with increasing temperature). As temperature increases conductivity σ shows transition from semiconducting -to- metallic at high frequency regime. The frequency dependence of conductivity σ in this sample is clear at high frequency. Increasing temperature, this

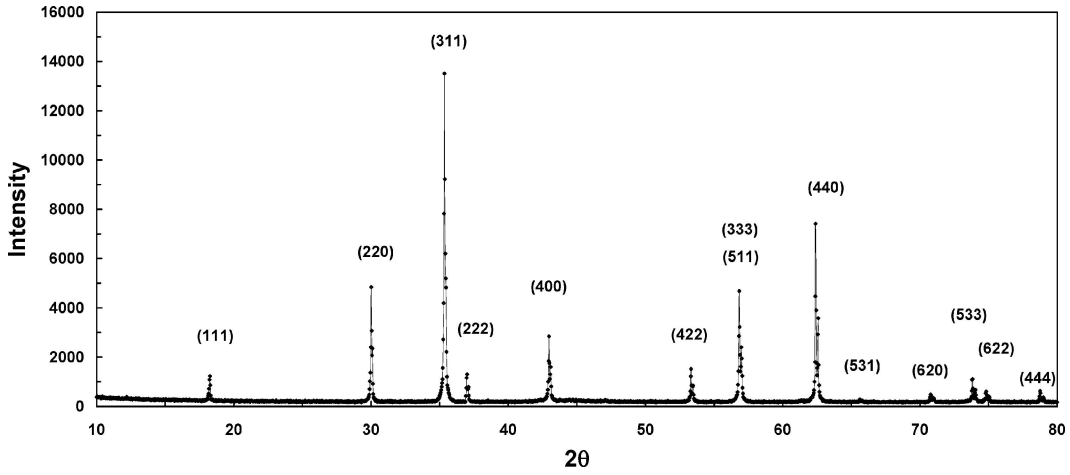

Figure 2 Step scan XRD pattern for $Cu_{1-x}Zn_xGa_{0.1}Fe_{1.9}O_4$ at room temperature.

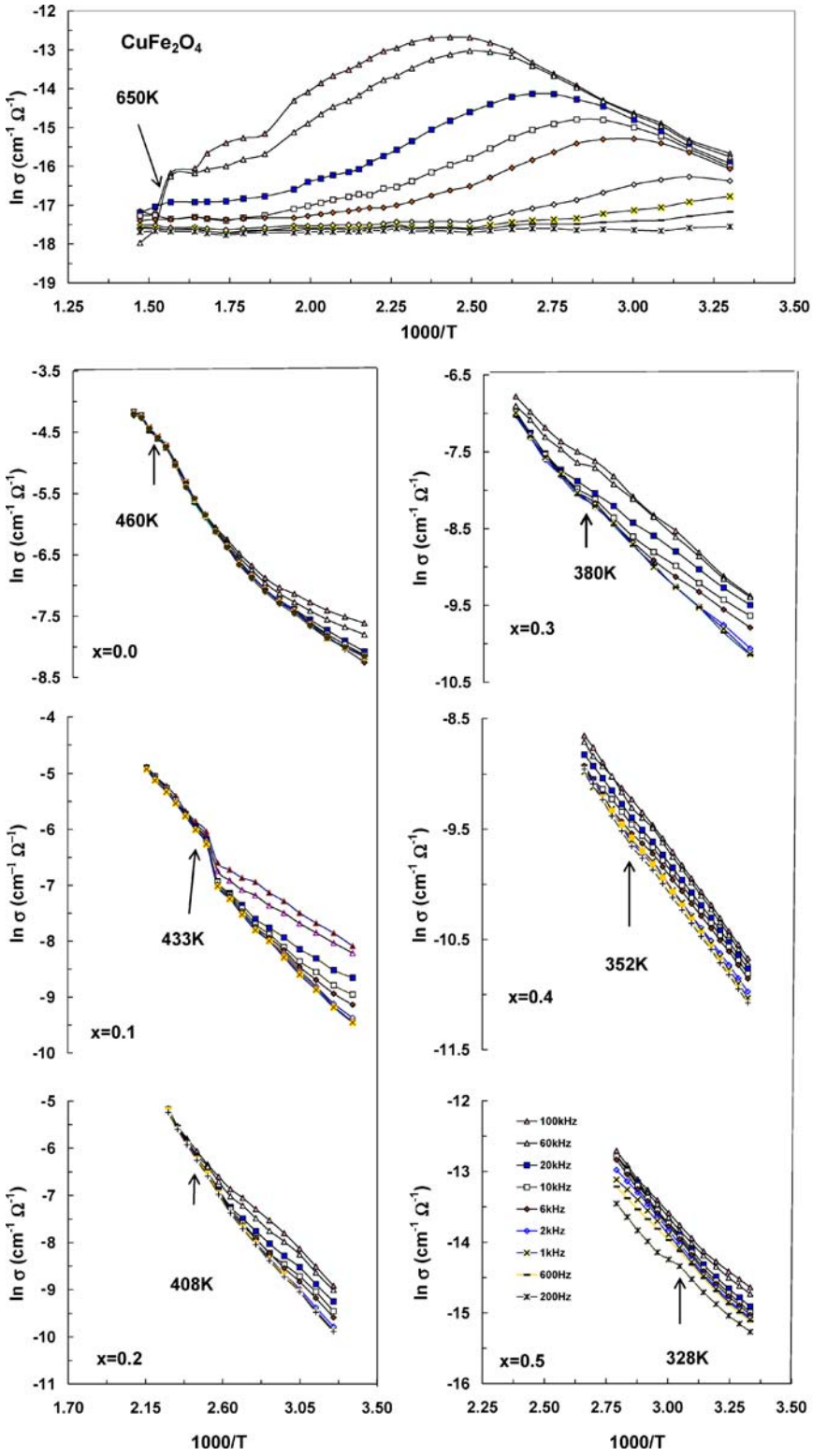

Figure 3 Conductivity as $\ln\sigma$ versus $1000/T$ for $CuFe_2O_4$ and $Cu_{1-x}Zn_xGa_{0.1}Fe_{1.9}O_4$ at different frequencies.

dependence decreases and conductivity σ becomes frequency independent at 650 K, which separates the ferrimagnetic region (where σ is frequency dependent) and the paramagnetic region (where σ is frequency independent) [20].

As Ga substitutes for Fe in $CuFe_2O_4$, the conductivity shows a semiconducting behavior (where, σ increases with increasing temperature). The frequency dependence of conductivity in this sample is clear at low range of temperature. In addition, the relation shows a change in the slope at temperature (460 K).

Replacing Zn instead of Cu in the $Cu_{1-x}Zn_xGa_{0.1}Fe_{1.9}O_4$ compound affects the dependence of conductivity on both temperature and frequency as follows:

At low Zn content $x = 0.1$ and 0.2, the conductivity shows frequency dependence at low temperature for different frequencies except the very low range where, σ nearly has a frequency independence at high temperature. The relation of σ with temperature for

TABLE III Cation distribution deduced from the X-ray analysis for the compositions $CuFe_2O_4$ and $Cu_{1-x}Zn_xGa_{0.1}Fe_{1.9}O_4$ with ($0.0 \leq x \leq 0.5$)

		Site		
Space group	Sample	(4a)	(8d)	(16h)
$I4_1/amd$	$CuFe_2O_4$	Fe^{3+}	Fe^{3+}, Cu^{2+}	O^{-2}
$I4_1/amd$	$CuGa_{0.1}Fe_{1.9}O_4$	Fe^{3+}	$Ga^{3+}_{0.1}$, $Fe^{3+}_{0.9}$, Cu^{2+}	O^{-2}
$I4_1/amd$	$Cu_{0.9}Zn_{0.1}Ga_{0.1}Fe_{1.9}O_4$	$Zn^{2+}_{0.1}$,$Fe^{3+}_{0.9}$	$Ga^{3+}_{0.1}$, $Fe^{3+}_{0.9}$, $Cu^{2+}_{0.9}$	O^{-2}
		(8a)	(16d)	(32h)
$Fd3m$	$Cu_{0.8}Zn_{0.2}Ga_{0.1}Fe_{1.9}O_4$	$Zn^{2+}_{0.2}$, $Ga^{3+}_{0.01}$,$Fe^{3+}_{0.79}$	$Ga^{3+}_{0.09}$,$Fe^{3+}_{1.11}$,$Cu^{2+}_{0.8}$	O^{-2}
$Fd3m$	$Cu_{0.7}Zn_{0.3}Ga_{0.1}Fe_{1.9}O_4$	$Zn^{2+}_{0.3}$, $Fe^{3+}_{0.7}$	$Ga^{3+}_{0.1}$,$Fe^{3+}_{1.2}$,$Cu^{2+}_{0.7}$	O^{-2}
$Fd3m$	$Cu_{0.6}Zn_{0.4}Ga_{0.1}Fe_{1.9}O_4$	$Zn^{2+}_{0.4}$, $Ga^{3+}_{0.02}$,$Fe^{3+}_{0.58}$	$Ga^{3+}_{0.08}$,$Fe^{3+}_{1.32}$,$Cu^{2+}_{0.6}$	O^{-2}
$Fd3m$	$Cu_{0.5}Zn_{0.5}Ga_{0.1}Fe_{1.9}O_4$	$Zn^{2+}_{0.5}$, $Ga^{3+}_{0.01}$,$Fe^{3+}_{0.49}$	$Ga^{3+}_{0.09}$,$Fe^{3+}_{1.41}$,$Cu^{2+}_{0.5}$	O^{-2}

these samples has remarkable changes at (433 and 408 K) for samples with $x = 0.1$ and 0.2 respectively.

As Zn content increases $x > 0.2$, the frequency dependence of conductivity is observed over the whole range of temperature and the relations show changes in slope at 380, 353 and 328 K for $x = 0.3$, 0.4 and 0.5 respectively.

The transition-metal cation at octahedral sites is interstices of an anion sublattice. The electrostatic interactions between anion and cation electrons cause splitting of cation $3d$-level into more stable triply degenerate t_{2g} level (d_{xy}, d_{yz}, d_{zx} atomic orbitals directed away from neighboring anions) and less stable, doubly degenerate e_g level (d_{z2}, d_{x2-y2} atomic orbitals directed towards neighboring anions) [21]. The factors that affect the interaction between any pair of cations are the relative coordination of their anion octahedral and the number of cation outer electrons.

Anderson [22] pointed out that if the cation–anion–cation angle is 90°, the predominant interactions are assumed to be cation–cation interactions, and when this angle is 180° or as small as 120°, the cation–anion–cation interactions is optimal. In addition, Goodenough [23], Ata-Allah and Fayek [24] and Ata-Allah [25] pointed out that in the rocksalt–type structure and spinel structure, both cation–anion–cation interactions and cation–cation interactions can be simultaneously presented. They also, stated that for $5 \leq m \leq 8$ (where, m is the number of electrons in $3d$-levels) the cation–anion–cation interaction must be stronger. In the case of strong cation–anion–cation interactions and weak cation–cation interactions, the materials have semiconductor (or insulator) behavior. However, if cations of same element but different valence are simultaneously present, the materials may have metallic type σ–T character below a ferromagnetic Curie temperature [23]. In case of strong cation–cation interactions between octahedral B-site cations, these materials have a metallic behavior and may become semiconductor at low temperature.

Compositions under investigation are transition–metal–oxide semiconductors with the spinel structure, which are known to be low–mobility materials. Their transport properties are arising from charge transfer between octahedral cations by hopping of localized d-electrons. This hopping mechanism is confined to the valence distribution of cations that occupy the oxygen octahedral site.

In the present materials, Cu^{2+} ions in the $CuFe_2O_4$ unit cell, are occupying the octahedral B-sites as reported earlier [17, 26, 27] and the cation distribution in this sample has the form $(Fe^{3+})[Fe^{3+}Cu^{2+}]O_4^{2-}$ [9] where the parenthesis refer to the tetrahedral A-site and square bracket refer to the octahedral B-site. While, Ga^{3+} and Zn^{2+} ions, due to their site preference [28], and Mössbauer studies on $Cu_{1-x}Zn_xGa_{0.3}Fe_{1.7}O_4$ [9] and from the crystallographic parameters estimated above are occupying the octahedral and tetrahedral in present compounds. Therefore, the cation–cation interaction [Cu^{2+}–Cu^{2+}] and the cation–anion–cation interaction between [Fe^{3+}–O^{2-}–Fe^{3+}] are predominant at the octahedral site in $CuFe_2O_4$ sample. The substitution of Ga^{3+} with a closed $3d$ shell ($3d^{10}$) in place of Fe at the octahedral B-site in $CuFe_2O_4$ decreases the number of [Fe^{3+}–O^{2-}–Fe^{3+}] interactions. In addition, the presence of Ga^{3+} at the B-site screens the [Cu^{2+}–Cu^{2+}] and [Fe^{3+}–O^{2-}–Fe^{3+}] interactions in this sample and lead to decrease the frequency dependence of conductivity as shown in Fig. 3. Substitution of Zn in place of Cu in this system, it replaces Fe at the tetrahedral site and leads to transfer more Fe ions to the octahedral site [9]. This increases the [Fe^{3+}–O^{2-}–Fe^{3+}] interactions and decreases the cation–cation interaction between Cu–Cu over the octahedral sites. This means that a strong cation–anion–cation interactions and weak cation–cation interactions, is present and leads to a semiconductor behavior as clearly shown in Fig. 3 in these compositions.

Fig. 4 shows the activation energies calculated from the relation between $\ln \sigma$ and $1000/T$ (Fig. 3) according to the equation $\sigma = \sigma_o \exp(-E/kT)$, where E is the activation energy and k is the Boltzmann's constant.

The relation shows the following remarks:

– The $CuFe_2O_4$ sample has a semiconductor behavior with positive temperature coefficient of conductivity (TCC) ($d\sigma/dt$) [29, 30] at low temperature range. While at high temperature range, the sample has a metallic behavior with negative TCC as illustrated in Fig. 3.

Samples with the compositional parameter ($0.0 \leq x \leq 0.5$) show a semiconducting behavior with positive TCC. The relation clearly shows that; as Zn replaces Cu in this unit cell the semiconductor behavior increases. This could be explained as;

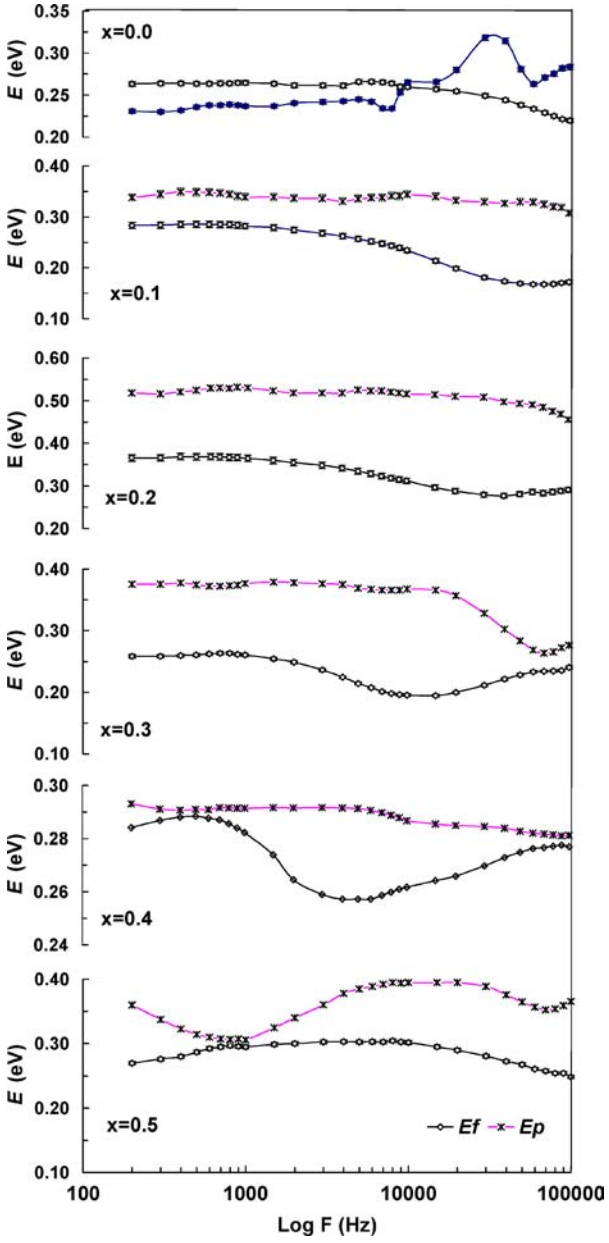

Figure 4 Plot of activation energy as a function of frequency for $CuFe_2O_4$ and $Cu_{1-x}Zn_xGa_{0.1}Fe_{1.9}O_4$ with x from 0.0 to 0.5 compounds.

– Compositions with high Cu content, Cu–Cu interactions have more contribution to the conductivity and leads to metallic behavior as in $CuFe_2O_4$ [18, 23].
– Substitution of Ga and Zn in the present unit cell, in one hand, decreases the Cu–Cu interactions where, on the other hand, the Fe–O–Fe interactions are the most predominant. This leads to the semiconducting behavior in these compositions [20, 22].

The common feature of semiconductors (and some disordered systems) is that the frequency-dependent of conductivity increases approximately linearly [31]. This feature can be seen in Fig. 5 where $\ln\sigma$ is plotted against $\ln\omega$; ($\omega = 2\pi f$).

In the present studied materials the total conductivity at a given frequency is considered as;

$$\sigma_{\text{total}}(\omega) = \sigma_{\text{o}} + \sigma(\omega) \tag{1}$$

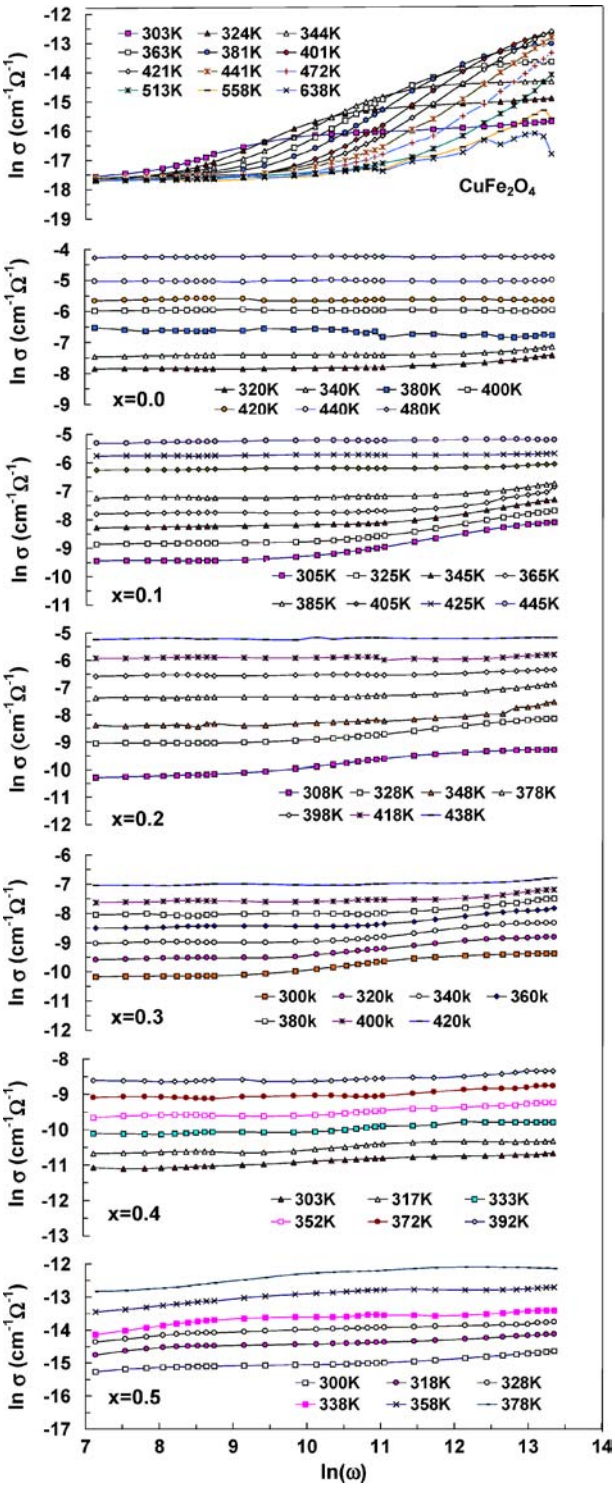

Figure 5 Conductivity as $\ln\sigma$ versus $\ln\omega$ for $CuFe_2O_4$ and $Cu_{1-x}Zn_xGa_{0.1}Fe_{1.9}O_4$ with x from 0.0 to 0.5 at different temperatures.

where σ_{o} is the dc conductivity due to band conduction and $\sigma(\omega)$ is the ac conductivity due to hopping conduction. The conductivity $\sigma(\omega)$ obeys the empirical formula of frequency dependence given by the ac power law: [32]

$$\sigma(\omega) = B(T)\omega^{s(T)} \tag{2}$$

where $B(T)$ is constant and the exponent $\mathbf{s}(T) \leq 1$.

The ac power law regime of the conductivity at high frequency has been widely observed in systems involving correlated hopping transport as for ionic

conduction. The behaviors of $\sigma(\omega)$ and s as a functions of both frequency and temperature when correlation effect are important as follows;

– The fractional exponent s is a measure of the degree of correlation between σ and frequency where, **s** should be zero for random hopping (i.e. σ is frequency independent) and tends to one as correlation increases (i.e. σ is frequency dependent).

– In general, the dependence of s on temperature is a function of the conduction mechanism. Qualitatively, small polarons (SP) are usually associated with increase in **s** with increasing temperature, while correlated barrier hopping (CBH) shows a decrease in s with increasing T. Overlap large polarons (OLP) show a linearly decreasing s with T reaching a minimum then start to increase again [32].

The results of $\ln\sigma$ versus $\ln\omega$ graph when fitted to the equation;

$$\ln\sigma = \ln B(T) + s\ln\omega \tag{3}$$

Yields a values of s and $\ln B(T)$ where their dependence on temperature is shown in Fig. 6. It is clearly shown that s decreases with increasing temperature for the $CuFe_2O_4$ sample in the low temperature range up to ~400 K. This means that the correlated barrier hopping (CBH) is the most predominant hopping mechanism in this sample. As Ga substitutes for Fe in this system the hopping conduction mechanism becomes OLP as indicated in Fig. 5 where s almost linearly decreases with T reaching a minimum then start to increase again. Substitution of Cu with Zn in the present system of ferrites, the CBH is present in the whole measured temperature range.

The variation of both s and $\ln B$ with temperature seems to be sensitive to the observed phase transformation. Anomalies in both s-T and $\ln B$-T relations are observed at the transition temperatures. Abrupt changes in s and $\ln B$ have previously been noted to occur at the transition temperature [T_C] from the magnetic region to the paramagnetic region [33].

These changes in both s-T and $\ln B$-T relations are coincides with that observed at the abrupt changes in the variation of the conductivity as $\ln\sigma$ with reciprocal of temperature as $(1000/T)$ at different frequency Fig. 3.

The transition temperature T_C determined from these relations Figs 3 and 6 is plotted against the compositional parameter x and displayed in Fig. 7. The relation shows that, substitution of Fe with Ga in

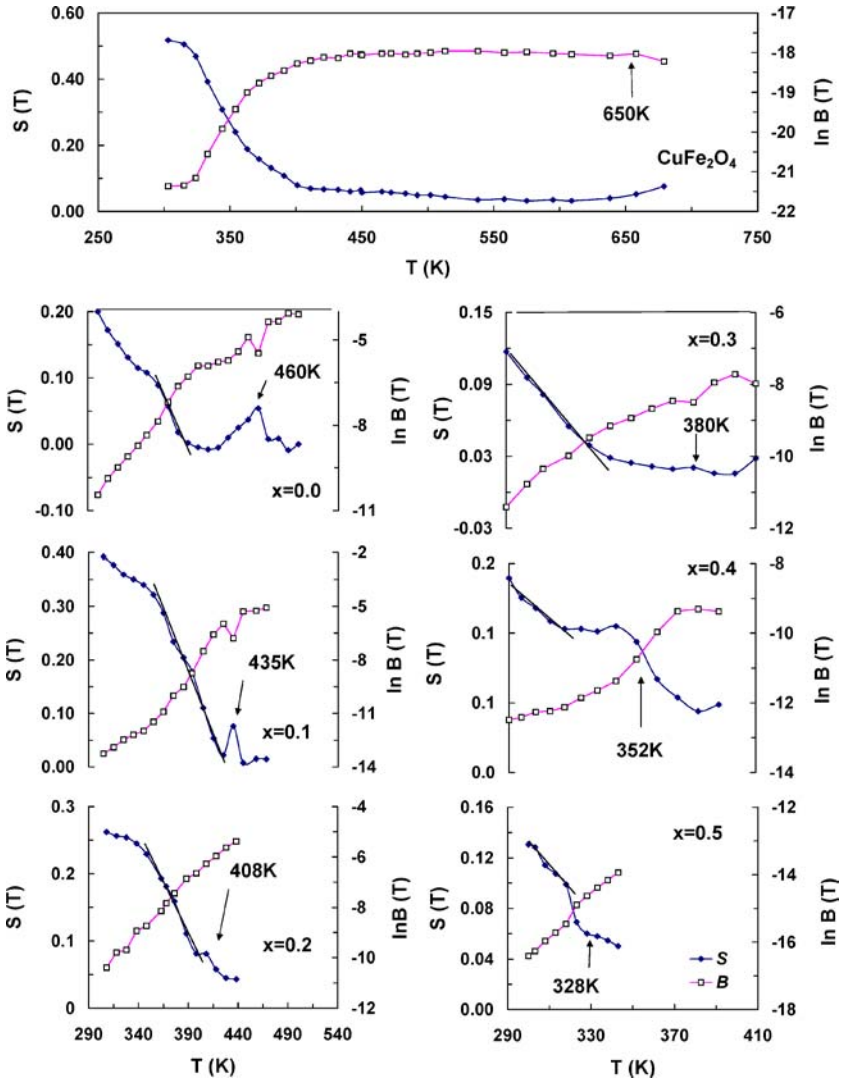

Figure 6 The relation of the universal exponent s and the pre-exponential $\ln B$ with temperature for $CuFe_2O_4$ and $Cu_{1-x}Zn_xGa_{0.1}Fe_{1.9}O_4$ with x from 0.0 to 0.5 samples.

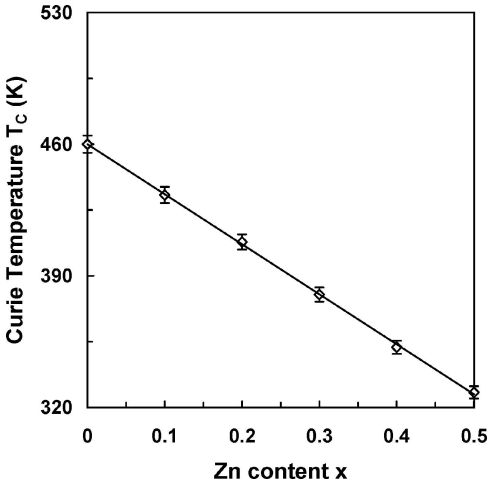

Figure 7 A plot of the transition temperature T_c with the compositional parameter x for $Cu_{1-x}Zn_xGa_{0.1}Fe_{1.9}O_4$ spinel ferrites.

$CuFe_2O_4$ decreases T_C from (650 to 460 K) and the substitution of Cu with Zn results in a linear decrease of T_C with zinc content x. This agrees with pervious studies for superexchange interaction for various oxides [9, 24, 25, 34], which indicated that the Curie temperature depends primarily upon the number of Fe^{3+}–O^{2-}–Fe^{3+} linkages. In our ferrite spinels $CuFe_2O_4$ and $Cu_{1-x}Zn_xGa_{0.1}Fe_{1.9}O_4$, T_C depends not only on the number of Fe^{3+} -O^{2-}–Fe^{3+} linkages at octahedral sites but also, upon the number of Fe^{3+}–$O^{2-}Fe^{3+}$ linkages at tetrahedral site. Replacement of Ga in place of Fe decrease these linkages at octahedral sites and the substitution of Cu with Zn decreases these linkages at tetrahedral sites and therefore transition temperature T_C is decreased.

4. Conclusion

From the obtained results and above discussions, it can conclude that: the metallic behavior is the most predominant in $CuFe_2O_4$ where cation-cation [Cu-Cu] interaction is major at B-sites. The semiconductor behavior is associated with compounds having Zn content, where cation–anion–cation [Fe–O–Fe] interaction is major at B-sites. In addition, over large polaron OLP and correlated barrier hopping CBH conduction mechanisms are presented in $CuFe_2O_4$ and $Cu_{1-x}Zn_xGa_{0.1}Fe_{1.9}O_4$ compounds respectively. The transition temperature T_C is decreased linearly with increasing Zn content.

References

1. K. J. STANDLEY, "Oxide Magnetic Materials" (Oxford Univ. Press, Clarendon, London/New York, 1972).
2. F. S. GALASSO, "Structure and Properties of Inorganic Solids" (Pergamon, Oxford, 1970).
3. E. W. GORTER, *Philips Res. Rep. Eindhoven* **9** (1954) 403.
4. G. BLASSE, *ibid.* **3**(Suppl.) (1964) and references therein.
5. T. MURASE, K. IGARAHI, J. SAWAI and T. NOMURA, *ICF7*, Bordeaux, France, (1996) vol. B3, p. 3.
6. C. P. POOLE and H. A. FARACH, *Z. Phys.* **B47** (1982) 55.
7. D. C. CARTER and T. O. MASON, *J. Am. Ceram. Soc.* **71** (1988) 213.
8. J. C. WAERENBORGH, M. O. FIGUEIREDO, J. M. P. CABROL and L. C. J. PEREIRO, *J. Solid State Chem.* **111** (1994) 300.
9. S. S. ATA-ALLAH, M. K. FAYEK and M. YEHIA, *J. Magn. Magn. Mater.* **279** (2004) 411.
10. W.A. DOLLAS and H.ST.C. O'NEILL, *Acta Cryst.* **C53** (1987) 657.
11. YU. KORCHAE, V. KAPUSTIANIK, R. TCHUURVINSKYI, Z. CZAPLA, S.DACRO and V. BAZHAN, *Phys. Stat. Sol. (b)* **228** (2001) 777.
12. XIAO-XIO TANG, A. MANTHIRAM and I. B. GOODENOUGH, *J. Solid Stat. Chem.* **79** (1989) 250.
13. P. J. WOJTOWICZ, *Phys. Rev.* **116** (1959) 32.
14. R. ENGLMAN and B. HALPERIN, *ibid.* **B2** (1970) 75.
15. G. SCHRODER and H. THOMAS, *Z. Phys.* **B25** (1979) 369.
16. M. ATANASOV, U. KESPER, B. L. RAMAKRISHNA and D. REINEN, *J. Sol. Stat. Chem.* **105** (1993) 1.
17. H. P. KIUG, and L. E ALEXANDER, "X-Ray Diffraction Procedures," 2nd ed. (Wiley, New York, 1974).
18. J. M. R. GONZALEZ and C.O. ARE Á N, *J. Chem. Soc. Dalton Trans.* **10** (1985) 2155.
19. E. DE GRAVE, J. DE SITTER and R. VANDENBERGHE, *Appl. Phys.* **7** (1975) 77.
20. M. K. FAYEK and S. S. ATA-ALLAH, *Phys. Stat Sol. (a)* **198** (2003) 457.
21. I. BUNGET, M. POPESCU, "Physics of Solid Dielectrics" (Editura Stiinsificâ Si Enciclopedicã, Bucharest, 1978).
22. P. W. ANDERSON, *Phys. Rev.* **79** (1950) 350.
23. J. B. GOODENOUGH, *ibid.* **6** (1960) 1442.
24. S. S. ATA-ALLAH and M. K. FAYEK, *J. Phys. Chem. Solids* **61** (2000) 1529.
25. S. S. ATA-ALLAH, *Mater. Chem. Phys.* **87** (2004) 378.
26. T. MURASE, K. IGARAHI, J. SAWAI and T. NOMURA, ICF7, Bordeaux, France (1996) Vol. B3, p. 3.
27. S. S. ATA-ALLAH and M. K. FAYEK, *Hper. Inter.* **128** (2000) 467.
28. XIAO-XIO TANG, A. MANTHIRAM and I. B. GOODENOUGH, *J. Solid Stat. Chem.* **79** (1989) 250.
29. S. S. ATA-ALLAH, YUNHUI XU and CH. HEIDEN, *Physica C* **221** (1994) 39.
30. YUNHUI XU, WEIYAN GUAN, S. S. ATA-ALLAH, and CH. HEIDEN, *ibid.* **235-240** (1994) 823.
31. A. K. J. JONSCHER, "Dielectric Relaxation in Solids," Chelsca Dielectric Press, Limited, London (1986).
32. S. R. ELLIOTT, *Adv. Phys.* **36** (1987) 135.
33. M. F. MOSTAFA, A. S. ATALLAH, *Phys. Lett. A* **264** (1999) 242.
34. M. A. GILLEO, *Phys. Chem. Solids* **13** (1960) 33.

Received 13 September
and accepted 20 December 2004